Ductile Fracture Behavior of AS4P Under Mixed Mode (I/II) Loading

Dong-Joon Oh*

Andong National University, Andong, 388 Song-Chon Dong, Kyungbuk 760-749, Korea

The aim of this study is to investigate the ductile fracture behavior under mixed mode (I/II) loading using SA533B pressure vessel steel. Anti-symmetric 4-point (AS4P) bending tests were performed to obtain the J-R curves under two different mixed mode (I/II) loadings. In addition, finite element analysis using Rousselier Ductile Damage Theory was carried out to predict the J-R curves under mixed mode (I/II) loadings. In conclusions, the J-R curves under Mixed Mode (I/II) loading were located between those of Mode I and Mode II loading. When the mixity of mixed mode (I/II) loading was high, the J-R curve of mixed mode (I/II) loading approached that of pure mode I loading after some amount of crack propagation. In contrast with the above fact, if the mixity was low, the J-R curve took after that of pure mode II loading. Finally, it was found that the predicted J-R curves made a good agreement with the test data through the tuning procedures of β values at the different mixed mode (I/II) loading.

Key Words : Mixed Mode (I/II) Loading, SA 533B Pressure Vessel Steel, Anti-Symmetric 4 Point (AS4P) Bending Test, Mixity, Rousselier Ductile Damage Theory (RDDT)

1. Introduction

In order to predict safe service life using Structural Integrity Methods, it is necessary to perform carefully controlled experiments to assess the characteristics of materials. However, many experimental studies using ductile material have shown that the data derived from small specimens tested in the laboratory have differed significantly from that of the full size structure. This problem has been a significant hindrance in the development of accurate predictive techniques for ductile fracture.

In addition to this, the vast majority of many studies performed on the ductile fracture have been in Mode I, whether or not this data can be used to assess the performance of cracked structures under general loading, which depends on the relative influence of other modes of crack tip response.

Therefore, this study examined the influence of mixed mode (I/II) response in an SA533B pressure vessel steel. To achieve this aim, Anti-Symmetric 4-Point bending test (AS4P) under mixed mode (I/II) loading was conducted and simulation using RDDT was also performed to predict the correspond J-R curves under mixed mode (I/II) loading.

* Corresponding Author,
E-mail : djoh@andong.ac.kr
TEL : +82-54-820-6016; **FAX** : +82-54-823-1766
Andong National University, Andong, 388 Song-Chon Dong, Kyungbuk 760-749, Korea. (Manuscript **Received** July 10, 2001; **Revised** January 31, 2002)

2. Experimental Method

2.1 Material

The material tested in this study was obtained from an SA533, Type B, Class 1 forged plate which was ductile to use for the power plant reactor. The heat treatments and the chemical compositions of SA533B/C1 are given in Table 1 and Table 2 respectively.

Three tensile specimens were used to determine the load vs. displacement curve to obtain values of 0.2% proof yield strength, the ultimate tensile strength and the Young's modulus and Poison's

Table 1 Heat treatment condition of SA533B/C1

Heat Treatment Condition	Temperature (℃)	Period	Cooling
Austenizing	870~908	4hr. 17min.	Water Quenching
Tempering	650~660	6hr. 40min.	Air Cooling

Table 2 Chemical compositions ($wt\%$) of SA533B/C1

C	Si	Mn	S	P	Cr	Mo	Ni	V	Cu
0.21	0.26	1.4	.018	.006	0.1	0.5	0.66	.003	0.04

Table 3 Tensile data of SA533B/C1

Yield Strength (MPa)	Ultimate Strength (MPa)	Young's Modulus (GPa)	Poison's Ratio
533.8	660.1	213.8	0.281

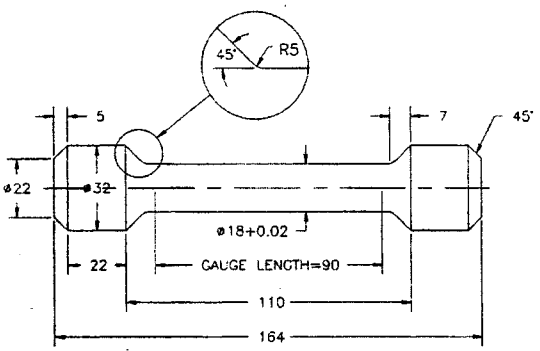

Fig. 1 Tensile specimen geometry

ratio (refer to Table 3). The diameter of tensile specimen was 18mm and the gauge length was 90mm The loading type of the tensile specimen was a shoulder end (Fig. 1) and the Schenck Machine (PM 250KN) was used.

2.2 Anti-Symmetric 4-Point Bending Test (AS4P)

The geometry of the test specimen was the same as the SECB specimen for the mode I test except the crack was eccentrically placed with reference to the centerline. Both the width and the thickness of the Anti-Symmetric 4-Point (AS4P) specimen was 25mm and the shape of section was rectangular to make the plane strain condition. Figure 2 shows the loading arrangement for AS4P loading with the corresponding shear force and bending moment diagram. Given that the bending moment, M, is associated with mode I and that the shear force, Q, is associated with mode II, it is evident that for the AS4P case the ratio of mode I to mode II varies with the position of the crack relative to the loading points. Along the center axis of the loading arrangement $M=0$, yet there is a substantial shear force, Q. Therefore, a crack positioned exactly on the central axis is loaded in pure Mode II. If the crack is positioned away from the center, Q remains constant and M increases and therefore the Mode I to Mode II ratio increases.

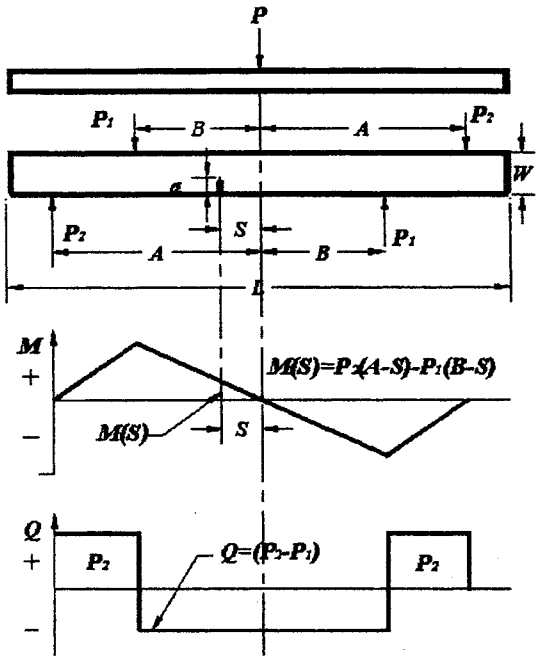

Fig. 2 Configuration of anti-symmetric 4-point bending test (AS4P)

In the AS4P arrangement, the fixture containing the specimen is subjected to a load per net thickness P that is offset by a distance S from the plane of the notch. From static equilibrium, we obtain

$$P_1=P\frac{A}{A+B}\quad P_2=P\frac{B}{A+B} \tag{1}$$

so that the plane of the crack is subjected to a shear force per unit thickness

$$Q=P_1-P_2=P\frac{A-B}{A+B} \quad (2)$$

While the moment across the crack plane is

$$M(S)=P_1(A-S)-P_2(B-S)=QS \quad (3)$$

The distances A and B and the loads P_1 and P_2 are identified in Fig. 2.

According to Wang *et al.* (Wang, 1977), K_I and K_{II} for this configuration are

$$K_I=\frac{M}{BW^{3/2}}Y_I,\ K_{II}=\frac{Q}{BW^{1/2}}Y_{II} \quad (4)$$

where W is the width of the plate, B is the plate thickness, and Y_I and Y_{II} are the mode I and mode II calibration functions, respectively. Note that the Y-calibrations are functions of the ratio of crack length to specimen width (a/W). However, since SECB specimens are widely used in pure Mode I fracture toughness test, Y_I has been determined with great accuracy by a number of independent investigators (Brown, 1966; Wilson, 1969). The results of these studies agree to within 1%. Wang *et al.* have determined Y_{II} by a boundary collocation method for $0,40<(a/W)<0.75$, and by a method which relates Y_{II} to Y_I. Two methods are found to agree within about±5%. The position of the crack, S, which gives the desired K_I/K_{II} can then be determined as

$$S=W\frac{Y_{II}}{Y_I}\tan\phi_{eq} \quad (5)$$

where $\tan\phi_{eq}=K_I/K_{II}$, and is a convenient measure of mode I/II loading.

In this study, tests were carried out at $\phi_{eq}=30°$ (close to mode II: $S=1.8$mm), and henceforth these specimens referred to as 'X-specimen' and the specimens tested at 60° (close to mode I: $S=5.5$mm) referred as 'Y-specimen'. The distance A, B was 80, 50mm, respectively. The loading positions were marked on the surface of the test specimens, with all measurements made relative to the crack tip.

All tests were carried out at room temperature using the hydraulic Schenck Universal testing machine of 250 KN capacity under a displacement control. A trace of load vs. load-displacement was recorded in order to evaluate the absorbed energy. Five specimens were used for each case in accordance with a multiple specimen method. The other procedures were based on the SECB test under Mode I loading condition. After finishing the test, the ligament parts of the AS4P specimens were brittle-fractured at a liquid nitrogen temperature (-196℃) and the crack lengths were physically measured using a travelling microscope.

To analyze the results of the mixed mode testing, a similar procedures which had adopted for the pure Mode I testing was introduced. The extraneous energy associated with the elastic compliance of the test fixture and any possibility of plastic deformation at the loading point was compensated by a supplement testing such as an unnotched specimen. This corrected area was then divided into its elastic and plastic components so that the method of η factors could be used to find J_e and J_p. The determination of mixed mode η factors is not usual and none have been calculated for the mixed mode (I/II) loading combination for AS4P test. After knowing the η factor, the mixed mode fracture toughness can be obtained from Eq. (6).

$$J=\frac{\eta_e U_e}{B(W-a)}+\frac{\eta_p U_p}{B(W-a)} \quad (6)$$

Unfortunately, due to the abrasive effect of two mating fracture surfaces under Mixed Mode loading, the load vs. load displacement curves could be overestimated. Its inaccuracy made it impossible to calculate the fracture toughness using Eq. (6). Therefore, the fracture toughness (J) was obtained using the direct comparison with the numerical analysis. After the FEM simulation to predict the crack growth using Rousselier damage theory was performed, the J values corresponding the same crack growth could be determined.

3. Simulation Using RDDT

The details of Rousselier Damage Ductile Theory (RDDT) are explained in references (Rousselier, 1987; Bilby, 1993). Briefly, the plastic potential (F) can be expressed as the sum of plastic potentials during the hardening (F_h) and the softening (F_s):

$$F=F_h+F_s=\frac{\sigma}{\rho}+\sqrt{3}B(\beta)De^{\frac{C\sigma_m}{\rho\sigma_Y}} \quad (7)$$

The damage function $B(\beta)$ can be determined from Eqn. (8)

$$B(\beta)=\sigma_Y f_0\frac{e^{\beta}}{C(1-f_0+e^{\beta})}$$
$$\beta=\ln\frac{f(1-f_0)}{f_0(1-f)} \quad (8)$$

where F : the plastic potential('h' subscript means hardening and 's' means softening)

σ_{eq} : the equivalent stress

ρ : the density

σ_m : the mean stress

σ_Y : the yield stress

β, C, D : the damage parameters can be determined by the following tune-up procedures and can not be fixed.

f, f_0 : the current and initial values of void volume fraction.

TOMECH was used as a tool to simulate the elastic-plastic finite element analyses using RDDT. This code was originally developed for this FEM simulation. For these analyses, some necessary parameters such as a mesh type and a size, mechanical properties, an inclusion volume fraction, the damage parameters of RDDT and the β constant for the criterion of damage should be determined.

A 4-node rectangular element was selected for this FEM analysis. Figure 3 shows the refined mesh for the X specimen using a critical mesh size (L_c=0.25mm) at the crack tip with the 10° inclined crack under Mixed Mode (I/II) loading. The critical mesh size was based on the distances of the inclusions such as MnS. These mean value was obtained from the direct measurement of the inclusion by the metallogrphy.

In this model where the inclined crack was going to move through the mesh, a regular and highly refined mesh, which covered the region of crack advance, was required to get more accurate results. For AS4P specimen, the crack was modeled as a line since the pre-fatigue crack was made. The angle of X specimens was 10° and that of Y specimens was 5° which was measured from the crack profiles using the image analyzer such

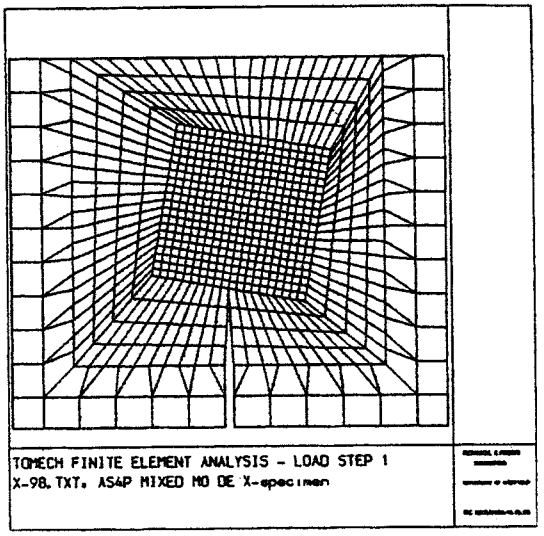

Fig. 3 Refined meshes for X-AS4P with crack angle 10°

as 'RepAn' system. Due to an anti-symmetry loading condition, the full geometries of the specimens were simulated.

Since an unwanted yielding took place beneath reaction points, small edges on reaction points were constrained in Y-direction in order to spread the load. A prescribed displacement was applied to small edges to load the specimen and the plane strain condition was assumed.

MnS volume fraction from the metallographic observation was so similar to that of Franklin's experimental equation that a metallographic value, 0.102%, could be used for this simulation. The true stress *vs.* true strain relationship used in the elastic-plastic analyses was determined experimentally and input to the code as 24 pairs of data points from the experimental curve.

The Rousselier's damage parameters C and D were initially tuned by simulating the load vs. notch root diametrical contraction curves of the round notch bar specimen [8]. These values of C (1.6) and D (2.0) were confirmed by the simulation of the J-R curves (Oh, 2000).

The β criterion was used for crack advance. If β value of the finite elements was over β_{crit}, these finite elements were considered as the damaged elements and removed from calculation. This crack advance method is called 'failed element

removal technique'. It was found in the previous study (Oh, 2001) that β_{crit}, depended on the type of loading condition such as mode I, or mode II loading by the comparison of J-R curves and the load *vs.* load-displacement curves.

4. Results and Discussion

4.1 Comparison of J-R Curves under Different Loading Condition

Figure 4 showed the J resistance curves under Mode I (○: SECB-25, ●: SECB-50, ★: V-notch), Mode II (□: SPS) and Mixed Mode (I/II) loading. J-R curves under Mode I and Mode II loading were obtained from the other studies (Oh, 2000 and 2001). While X-specimen (ϕ_{eq}=30°) close to Mode II loading (ϕ_{eq}=0°) was denoted as △, Y-specimen (ϕ_{eq}=60°) close to Mode I loading (ϕ_{eq}=90°) was marked as ▲.

Figure 4 showed that while the fracture toughness under Mode I loading was the highest, the J resistance curve under Mode II loading was the lowest. Other studies have shown that the mode II fracture resistance value could be significantly greater than (Singh, 1989; Banks-Sills, 1986) comparable with (Suresh, 1987) or smaller than (Davenport, 1993) that in mode I. These results were consistent with Davenport's results. The underlying causes of these differences are presently obscure.

From Fig. 4, the Mixed Mode results lay between these two curves under Mode I and Mode II loading. The fracture toughness of Y specimens (close to Mode I: ϕ_{eq}=60°) is higher than that of X specimen (close to Mode II: ϕ_{eq}=30°). In other words, the fracture resistance decreases as the component of Mode II loading is increased.

Davenport has attempted to obtain a simple relationship between the Mode I and Mode II loading characteristics of SA508 steel. He has used an interpolation between the Mode I and II load-line results but it was found that his interpolation method was not adequate for this study to model the behavior of SA533B steel since the J resistance curve of Y specimen represented S-shape curve (Fig. 4, ▲). J-R curves under Mixed Mode loading (I/II) showed that these

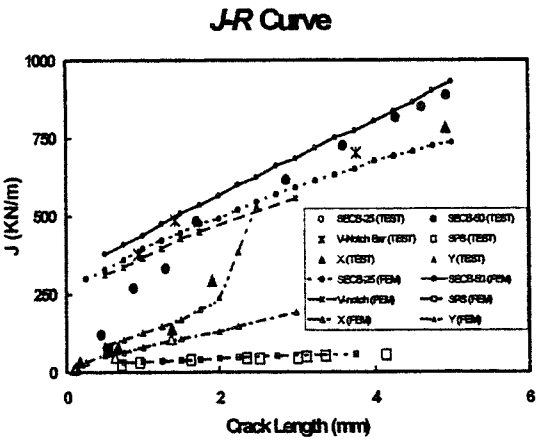

Fig. 4 Comparison of J resistance curves obtained from tests and simulations under different mixed mode (I/II) loading (X: ϕ_{eq}=30°, Y: ϕ_{eq}=60°)

curves were close to that of Mode II loading at the initiation of cracking and it implied that the mechanisms of Mixed Mode (I/II) was similar to that of Mode II during the crack initiation. After some amount of crack extended, the resistance curves changed depending on the mixity of loading.

4.2 Prediction of ductile fracture using RDDT

Modeling using Damage Mechanics has provided some insight, as was demonstrated in Fig. 4. The J resistance curves of Mode I and Mode II loading from test results were in a reasonable agreement with the predicted J-R curves using RDDT which were marked as lines with the corresponding symbols.

Figure 4 also showed the predicted J resistance curves obtained using the contour J integral under two different Mixed Mode (I/II) loading. They are compared with those obtained from Mode I and Mode II loading tests. While the tested and predicted J resistance curves of X specimen (close to Mode II) showed straight lines, those of Y specimen (close to Mode I) approached to the J resistance curve under Mode I loading as the crack extension was over 2mm. The two predicted J resistance curves under Mixed Mode loading (I/II) also made a good

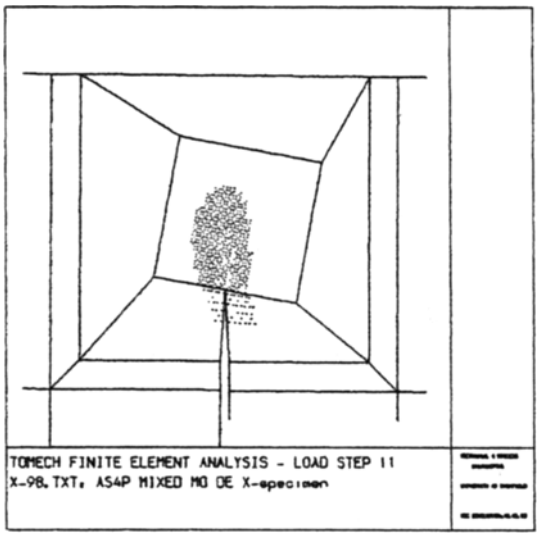

Fig. 5 Plastic zone shape for X- AS4P ($\phi_{eq}=30°$)

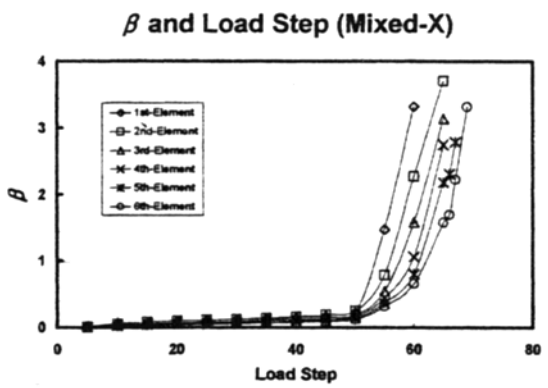

(a) $\beta_{crit}^{X}=2.5$

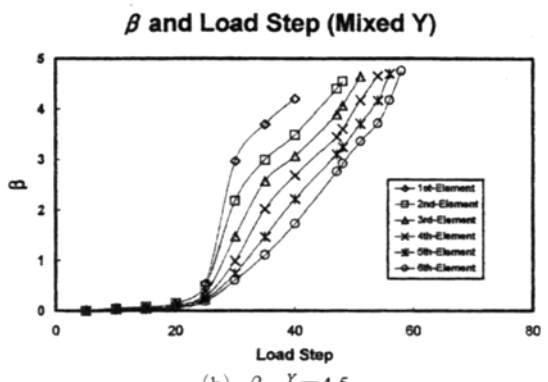

(b) $\beta_{crit}^{Y}=4.5$

Fig. 6 β Variation under mixed mode (I/II) loading

agreement with the test results and were located between that of Mode I loading and that of

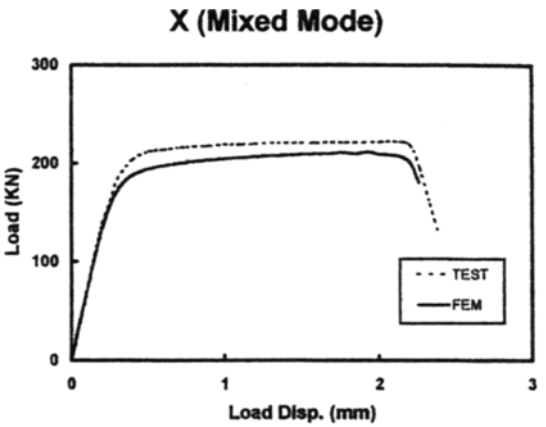

(a) X specimen

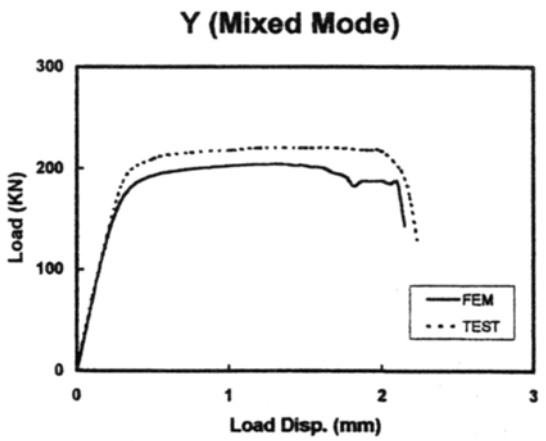

(b) Y-Specimen

Fig. 7 Comparison of load *vs.* load displacement curves between simulation results and test data under mixed mode (I/II) loading

Mode II loading. As the mixity of loading (ϕ_{eq}) was increased (approach to Mode I loading), the J resistance was also increased.

It was clear that the J-R curves under Mode II loading was lower than that under Mode I loading and the those under Mixed Mode (I/II) were located between them.

To evaluate the FEM analysis using RDDT, the followings were reviewed. First, the plastic zone shape of X-specimen under mixed mode (I/II) loading which is close to Mode II loading, was displayed in Fig. 5. The shape became similar to that of Mode II loading. In the case of Y-specimen, the plastic zone shape became less similar to Mode II loading than that of X-specimen.

Secondly, through the tuning-up procedures of the β-damage value for mixed mode I/II loading, new β_{crit}^{X} and β_{crit}^{Y} were determined as 2.5 and 4.5 respectively. While the β_{crit}^{X} value for X specimen was 2.5 which was larger than that for Mode II loading, β_{crit}^{Y} for Y specimen was 4.5 which was less than that for Mode I loading.

As the load was increased, β values of the first six elements in front of the crack tip were changed in Fig. 6. After the β value of the first element was over β_{crit} and the load was increased, the remaining elements approached to β_{crit} in turn.

Figure 7 illustrates the load versus load displacement relation and since there was some abrasive action between two mating fracture surfaces, load versus load displacement curve taken from Mixed Mode test was deviated from the predicted one.

The previous study (Oh, 1999) showed that the general fracture mechanism for ductile material under Mixed Mode (I/II) loading conditions was microvoid nucleation, growth and coalescence. It was possible to model microvoid nucleation and growth using a continuum damage theory (Rousselier, 1987; Bilby, 1993) which gave a dilatational plasticity leading to softening with increasing deformation. In such a modeling of ductile material, there was no attempt to model in details the void coalescence or final material failure. Instead, the crack growth or the crack position was identified by the attainment of the critical values of the damage parameter, β, in the Rousselier model which indicated the history of loading (Howard, 1994a, 1994b).

While the test J resistance curves of Mode I, Mode II loading and the X specimen (close to Mode II: $\phi_{eq}=30°$) agreed with the predicted one, that of Y specimen (close to Mode I: $\phi_{eq}=60°$) shows a small deviation from the predicted one. It was believed that the abrasive effect of both rubbing fracture surfaces under Mixed Mode loading could lead to the overestimated load versus load displacement relation (Fig. 5). In addition, since the shear deformation process took place rapidly at the microvoid coalescence stage, the corresponding crack length and the current load could not be measured accurately.

When the crack under mixed mode (I/II) loading initiated, the toughness of Mixed Mode loading was relatively very lower than that of Mode I loading but a little higher than that of Mode II loading. As the crack grew over 2mm, the J resistance curve of Y specimen raised steeply until the J resistance curve of Mixed Mode approached to that of Mode I loading. It implied that the effect of loading condition was changed during the crack extension. It was also related to the microvoid fracture mechanism of Mixed Mode loading. The fractographs (Oh, 1999) taken by SEM supported this assumption: the fractograph of Y specimen at the crack initiation stage showed the elliptical dimple shape which was similar to that of Mode II loading. As crack extended, the oval dimple shape with direction was observed which was similar to that of Mode I loading. In other words, the fracture mechanism of Y specimen was gradually changed from Mode II loading to Mode I loading.

4.3 Effect of damage parameter, β

With the usual hypothesis of a constant volume plastic deformation, it is generally possible to ignore the variation of density, but if the ductile damage theory is adopted the variation of density should be considered. If there is no damage, density (ρ) will be constant and the only change of density is small due to elastic deformation. If ρ is variable, the variation of β depends on the density. Consequently, as a first approximation of Rousselier damage theory, it was assumed that

$$\beta=\beta(\rho) \tag{9}$$

Li *et al.* (Li, 1994) showed that expression for β was very similar to the void growth ratio R/R_0 given by the integration of the average rate of void growth (Rice, 1969) and they , therefore, expected predictions using β and $\ln(R/R_0)$ as criteria for crack advance to be similar. A physical connection between β and the void growth was indicated by their studies and they also claimed that a criterion for crack advance controlled by the attainment of a specific value of β was connected with the growth of voids to a specific size.

In previous studies (Oh, 2001), the attempt to use the same critical value of β as that obtained from tuning of the Mode I loading in order to predict the ductile fracture behavior under Mode II loading had been made; unfortunately, this attempt did not predict the observed fracture resistance under Mode II loading properly. It was found that the predicted J resistance curve using the β^I value of Mode I loading was higher than the test data of Mode II loading and the softening of the materials took place slower than the test data. After tuning the critical β value of Mode II loading, β_{crit}^{II}, it was discovered that the β value of Mode II was smaller than that of Mode I.

In addition, it was expected and confirmed that the β values of Mixed Mode were also between those of Mode I and Mode II and the variation of β value was related to the mixity of different loading. Table 4 showed the β value versus mixity of Mode I and Mode II loading and Fig. 8 demonstrated that the critical β value varied linearly with the mixity defined as the equivalent crack angle (Eq. (10)).

$$\phi_{eq}=\tan^{-1}(K_I/K_{II}) \tag{10}$$

It was believed that the reason of the variable

Table 4 β Value at different loading condition

Mixity $\phi=\tan^{-1}(K_I/K_{II})$	Mode II(0°)	Mixed (30°)	Mixed (60°)	Mode I (90°)
β_{crit}	1.5	2.5	4.5	5.5

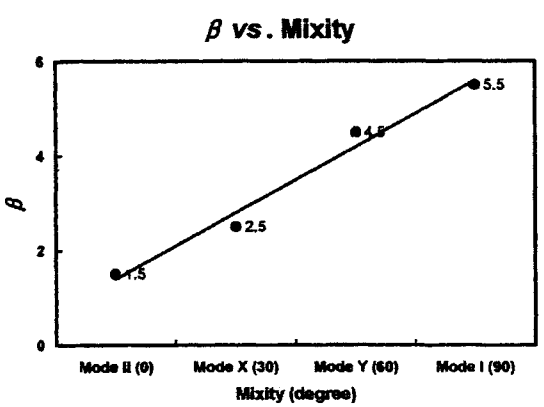

Fig. 8 β values versus mixity, $\phi=\tan^{-1}(K_I/K_{II})$, under different loading: (ϕ=90° for Mode I and ϕ=0° for Mode II)

β values at the different loading condition was closely related to the microvoid fracture mechanism of ductile materials. That is, different microvoid fracture mechanisms produced different critical β values. This study suggested that the critical value of the damage parameter, β_{crit}, was constant for a particular loading condition and it was practical to classify the fundamental ductile damage parameters such as β_{crit}^I, and β_{crit}^{II}. For Mixed Mode (I/II) loading, prediction could be made with a combined parameter (refer to Fig. 8):

$$\beta_{crit}^{Mix}=f(\beta_{crit}^I, \beta_{crit}^{II}, mixity) \tag{11}$$

5. Conclusions

The ductile fracture behavior under Mixed Mode (I/II) loading using A533B/C1 pressure vessel steel was investigated. Experiments of AS4P and the prediction of RDDT were performed simultaneously. By the comparison between the test data and the predicted results, the following conclusions were obtained,

(1) While J-R curve under Mode I loading was the highest and Mode II the lowest, J-R curves under Mixed Mode (I/II) loading were located between those of Mode I and Mode II loading. For the Y specimen (close to Mode I loading: ϕ_{eq}=60°), the toughness at crack initiation was very low and J-R curve was located at the close to those of Mode II loading. After some amount of crack growth, J-R curve of Y specimens approached to those of Mode I loading. It implied that the micromechanism was changed from Mode II to Mode I as the crack grew.

(2) It was found that by new tuning of β values at the different mixed mode (I/II) loading, the predicted J-R curves made a good agreement with the test data. It was also discovered that the critical damage parameter, β_{crit}, was the function of loading type and it could be classified by β_{crit}^I, β_{crit}^{II}, and $\beta_{crit}^{MIx(I/II)}$ depending on the loading condition. The damage parameter, β, was proportional to the mixity of loading. While β_{crit}I and β_{crit}II were 5. 5 and 1. 5 respectively, the values of $\beta_{crit}^{MIx(I/II)}$ were in the range from 4.5 to

2.5 depending on the mixity of loading.

References

Banks-Sills, L. and Bortman, Y., 1986, "A Mixed-mode Fracture Specimen: Analysis and Testing," *International Journal of Fracture*, 30, pp. 181~201.

Bilby, B. A., Howard, I. C. and Li, Z. H., 1993, "Prediction of the First Spinning Cylinder Test Using Ductile Damage Theory," *Fatigue and Fracture of Engineering Materials and Structures*, 16, pp. 1~20.

Brown, W. F. and Srawley, . ., 1966, "Plane Strain Crack Toughness Testing of High Strength Metallic Materials," ASTM STP 410 pp. 1~129.

Davenport, J. C. W., 1993, "Mixed Mode Elastic-Plastic Fracture," Ph. D. Thesis, University of Bristol.

Howard, I. C., Li, Z. H. and Bilby, B. A., 1994a, "Ductile Crack Growth Predictions for Large Centre Cracked Panels by Damage Modelling Using 3-D Finite Element Analysis," *Fatigue and Fracture of Engineering Materials and Structures*, 17, pp. 959~969.

Howard, I. C., Li, Z. H. and Bilby, B. A., 1994b, "Ductile Fracture Prediction of Large Centre-Cracked Panels by Damage Theory Using 3-d Finite Element Calculations," *Fatigue and Fracture of Engineering Materials and Structures*, 17, pp. 1075~1087.

Li, Z. H., Bilby, B. A. and Howard, I. C., 1994, "A Study of the Internal Parameters of Ductile Damage Theory," *Fatigue and Fracture of Engineering Materials and Structures*, 17, pp. 1075~1087.

Oh, D. J., 1999, "Ductile Fracture Behaviour under Mixed Mode (I/II) Loading," Ph. D. Thesis, University of Sheffield.

Oh, D. J. et al., 2000, "Ductile Fracture Behaviour under Mode I Loading Using Rousselier Ductile damage Theory," *KSME Int. Journal*, Vol. 14, No. 9, pp. 978~984.

Oh, D. J., 2001, "Ductile Fracture Behavior of SPS Specimen under Pure Mode II Loading," *Journal of KSME(A)*, Vol. 25, No. 2, pp. 289~295.

Rousselier, G., 1987, "Ductile Fracture Models and Their Potential in Local Approach of Fracture," *Nuclear Engineering and Design* 105, pp. 97~111.

Rice, J. R. and Tracey, D. M., 1969, "On the Ductile Enlargement of Voids in Triaxial Sstress Fields," *Journal of Mechanics, Physics and Solids*, 17, pp. 201~217.

Singh, D. and Shetty, D. K., 1989, "Fracture Toughness of Polycrystalline Ceramics in Combined Mode I and Mode II Loading," *Journal of American Ceramic Society*, 72, pp. 78~84.

Suresh, S. and Tschegg, E. K., 1987, "Combined Mode I-Mode III Fracture of Fatigue-Precracked Alumina," *Journal of American Ceramic Society*, 70, pp. 726~733.

Wang, K. J., Hsu, C. L. and Kao, H., 1977, "Calculation of Stress Intensity Factors For Combined Mode Bend Specimens," *Fracture 1977*, Vol. 4, ICF4, Waterloo, Canada

Wilson, W. K., 1969, "On Combined Mode Fracture Mechanics" Westinghouse Research Labs Report 69-1E7-FMECH-R1 1